Taylor & Francis
Taylor & Francis Group

RESEARCH ARTICLE

OPEN ACCESS | Check for updates

Inactivated mycobacterium paragordonae delivered via microneedle patches as a novel tuberculosis booster vaccine

Moonsu Lee[a], Dohyeon Jeong[a], Kiyoung Yoon[a], Juyoung Jin[a], Yong Woo Back[b], In-Taek Jang[b], Hwa-Jung Kim[c], Bum-Joon Kim[d], and Sung Min Bae[a]

[a]Medical Business Division, Raphas Co, Ltd, Seoul, Republic of Korea; [b]R&D Center, Myco-Rapha Inc, Daejeon, Republic of Korea; [c]Department of Microbiology and Medical Science, College of Medicine, Chungnam National University, Daejeon, Republic of Korea; [d]Department of Microbiology and Immunology, College of Medicine, Seoul National University, Seoul, Republic of Korea

ABSTRACT

Tuberculosis (TB) remains a significant global health challenge with approximately 8.2 million new cases reported in 2023, despite the century-old Bacillus Calmette-Guérin (BCG) vaccine. BCG's protective efficacy diminishes over time, especially against pulmonary TB in adults. This study evaluates ethanol-inactivated *Mycobacterium paragordonae* (*M.pg*) delivered via Microneedle Array Patches (MAPs) as a novel booster strategy to enhance BCG vaccination efficacy. Various inactivation methods including heat treatment, formalin, and ethanol were compared, with ethanol-inactivated *M.pg* selected for optimal preservation of morphology and immunologically significant proteins. MAPs were fabricated using the droplet extension technique (DEN). Immunological assessment was conducted in a mouse model receiving either BCG alone or BCG followed by one or two administrations of inactivated *M.pg* MAP. Protective efficacy was evaluated through *M. tuberculosis* H37Rv challenge. Ethanol inactivation uniquely preserved morphology and maintained protein integrity, particularly Ag85B. Two administrations of inactivated *M.pg* following BCG priming significantly enhanced protective immune responses compared to BCG alone, inducing strong Th1-polarized immunity characterized by elevated IFN-γ, TNF-α, and IL-2 production in both CD4+ and CD8+ T cells. This vaccination strategy effectively generated effector memory T cells in lung and spleen, contributing to significant reduction in bacterial burden following challenge, with the BCG+Inactivated M.pg[2nd] group demonstrating the greatest reduction. Inactivated *M. pg* delivered via microneedle patches represents an effective booster strategy for enhancing BCG-induced protection against tuberculosis, with a two-dose schedule demonstrating optimal efficacy. This approach combines the safety advantages of an inactivated vaccine with the practical benefits of MAPs, addressing key limitations of tuberculosis vaccination strategies.

Introduction

Tuberculosis (TB) remains a significant global health challenge, with the World Health Organization (WHO) reporting approximately 8.2 million new TB cases in 2023, the highest number since global TB monitoring began in 1995.[1] The persistent increase in the prevalence of this disease underscores its significant and ongoing threat to public health, as detailed in this report. The Bacillus Calmette-Guérin (BCG) vaccine, despite nearly a century of use, remains the sole licensed vaccine for tuberculosis (TB) prevention.[2] Although BCG has proven effective in mitigating severe forms of TB in pediatric populations, its protective efficacy diminishes over time, especially against pulmonary TB, the predominant form of the disease in adults.[1,3,4] Moreover, its protective effect typically lasts only 10–20 years.[5]

A prime-boost vaccination strategy has been explored as a potential method to augment BCG effectiveness; however, the impact of BCG revaccination with repeated doses shows limited efficiency.[6] A novel approach to address these limitations involves utilizing *nontuberculous mycobacteria* (NTMs) to augment the protective efficacy of the BCG vaccine. This strategy has research as a method for enhancing tuberculosis prevention, leveraging the potential synergistic effects between NTMs and the existing BCG vaccination protocol. Inactivation of NTMs is commonly employed in these vaccines to ensure safety while maintaining immunogenicity. DAR-901, an inactivated *Mycobacterium obuense* strain derived from SRL172, has shown promising results in Phase 1 trials as a BCG booster tuberculosis vaccine.[7,8] In addition, non-tuberculous bacteria *Mycobacterium avium* is a vaccine candidate for TB. Oral live *M. avium* post-BCG reduced protection, while intraperitoneal killed *M. avium* enhanced it. This model provides a platform for evaluating novel tuberculosis vaccines.[9,10]

Mycobacterium paragordonae (*M.pg*), the NTM closely related to *Mycobacterium gordonae* (99.0% sequence similarity), was first isolated from the lungs of a patient in South Korea in 2014.[11] A previous study reported a novel

mycobacterial species phenotypically and genetically closed to *Mycobacterium gordonae*, but distinguished by its atypical growth temperature requirements, with an optimal range of 25–30°C and no growth at 37°C.[11] *M.pg* has emerged as a promising tuberculosis vaccine candidate, demonstrating enhanced protective immune responses compared to BCG in mouse models, with studies showing it induces stronger cell-mediated immunity characterized by increased IFN-γ production, improved T cell activation, and a more robust Th1-type immune response.[12] Furthermore, *M.pg* has shown potential as a vaccine vector for various pathogens, including HIV-1 and SARS-CoV-2, by eliciting enhanced pathogen-specific immune responses when used as a recombinant expression system.[13,14]

Microneedle arrays patch (MAP), comprising a multitude of micron-scale needles, offer a compelling alternative for transdermal vaccine delivery, bypassing the pain associated with traditional injections.[15–17] Compared to conventional intramuscular and subcutaneous injections, microneedles present a range of advantages.[18–20] These diminutive needles, typically ranging from 25 to 1000 μm in length, efficiently target antigen-presenting cells, such as Langerhans cells and dendritic cells, within the epidermis and dermis, thereby eliciting robust immune responses.[21–23] The skin's epidermal and dermal layers, rich in immune components, offer a compelling target for vaccine delivery.[18,24] Furthermore, the patch-like format of microneedle arrays facilitates ease of administration, eliminates the necessity for cold-chain storage, and enables self-administration, addressing critical logistical challenges associated with traditional vaccination approaches.[22,23,25]

In this study, we evaluated the efficacy of an inactivated *M.pg* strain as a microneedle vaccine, aiming to provide a safer alternative to the BCG vaccine. While previous research demonstrated the immunogenic potential of microneedle vaccines using live *M.pg* bacteria,[26] inactivated *M.pg*-based vaccines were not assessed. Inactivated vaccines offer a superior safety profile compared to live vaccines, potentially mitigating unforeseen complications. Therefore, an inactivated *M.pg* MAP vaccine could serve as a promising booster vaccine candidate for tuberculosis, enhancing safety and contributing to improved vaccination strategies.

Materials and methods

Preparation of inactivated M.Pg

The *M.pg* strain was grown at 30°C in MO-3SD (In house medium). *M.pg* was harvested by centrifugation at 2500 × g for 20 minutes and washed twice in PBS. Before inactivation, ten-fold serial dilutions were prepared and plated in agar-solidified 7H9 with OADC in quadruplicate to assess the number of cfu in the *M.pg*. PBS resuspended *M.pg* was then inactivated in a water bath at 80, 90 and 100°C for 30 minutes. In the case of formalin and ethanol inactivation, *M.pg* culture was incubated with 0.4% (vol/vol) formalin and 70% (vol/vol) ethanol during 30 min. *M.pg* viability was checked for each treatment *M.pg* by counting colonies from 7H10-OADC agar plates and using

a bacterial cell counter (QUANTOM Tx™, Logos Biosystems, South Korea). Morphology of *M.pg* was assessed via Scanning electron microscopy (SEM) following negative staining. Western blot analysis with anti-Ag85B (Myco-Rapha, Daejeon, Rep. of Korea) was performed to determine the protein profile.

Fabrication of M.Pg microneedle array patch vaccine

Dissolving microneedle array patch (MAP) containing the live and inactivated *M.pg* were fabricated using the DEN (droplet extension technique) method. In this technique, droplets were solidified and formed into cone shape microstructure by air blowing, as previously described. The MAP used in this study was fabricated by Raphas Co., Ltd. (Seoul, Rep. of Korea). Live and inactivated *M.pg* MAP, 25 base arrays in 1.6 cm X 1.6 cm (2.56 cm^2) for 1×10^6 pfu of patch, respectively. All patches were dispensed onto a pattern-mask hydrocolloid adhesive sheet (Hiks C&T, Rep. of Korea) using a customized MPP-1 dispenser (Musashi Engineering, Inc., Tokyo, Japan) with 10% hyaluronic acid (HA, Kikkoman Biochemifa Company, Tokyo, Japan). The dispensed array was then dried overnight at room temperature. The two dispensed droplets were brought into contact and extended to the target length, and then symmetric air blow was applied at room temperature to solidify the extended viscous droplets, forming cone-shaped microstructures. The mechanical strength of each MAP was measured using the universal test machine (UTM, ZwickRoell GmbH & Co. KG, Ulm, Germany). For final packaging, each MAP was placed in a polyethylene terephthalate (PET) blister pack (thickness: 280 μm); the blister pack was sealed in light-protective foil pouches (thickness: 100 μm) with desiccant.

Mice

Specific-pathogen-free (SPF) female C57BL/6 mice, aged 6–8-weeks were purchased from Nara Biotech (Seoul, Rep. of Korea) and used in our study. All animals were housed at the preclinical Research center of Chungnam National University Hospital (Daejeon, Rep. of Korea) and fed on sterile food and water ad libitum. The experiments were performed in accordance with the approval of the Institutional Research and Ethics Committee at Chungnam National University (approval number: CNUH-2022-IA0115) and the Korean Food and Drug Administration.

Vaccination

Two vaccination experiments were conducted using female C57BL/6 mice (6 weeks old), with 5 mice allocated to each experimental group (Figure 1s). In one experiment, mice received either one (Inactivated Mpg^{1st}) or two (Inactivated Mpg^{2nd}) applications of an Inactive *M.pg* MAP (1×10^6 cells/ patch) at 2-week intervals, a single (Live Mpg^{1st}) application of a Live *M.pg* MAP (1×10^6 cells/patch), or a single intradermal injection of Live *M.pg* MAP (1×10^6 cells/50 μL). In a separate experiment, mice were first subcutaneously
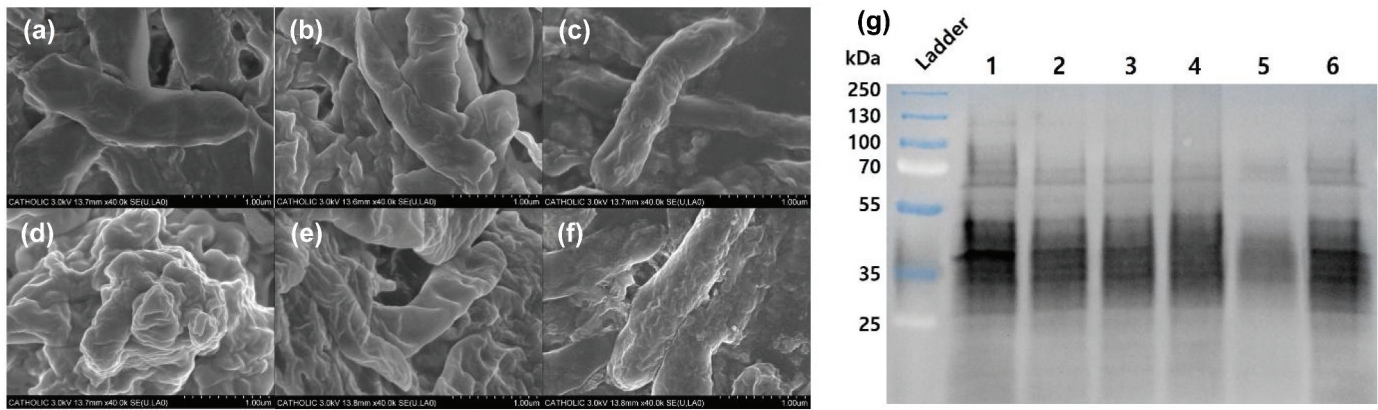
Figure 1. Morphological and molecular changes in *M.pg* under different treatments. (a–f) Scanning electron microscopy (SEM) images of *M.pg* subjected to various treatments: (a) untreated *M.pg*, (b) MPG treated with heat at 80°C, (c) *M.pg* treated with heat at 90°C, (d) *M.pg* treated with heat at 100°C, (e) *M.pg* treated with 4% formalin, and (f) *M.pg* treated with 70% ethanol. Scale bar = 1 μm. (g) SDS-PAGE analysis of protein profiles from *M.pg* under the same treatments: Lane 1, untreated *M. pg*; Lane 2, *M.pg* treated with heat at 80°C; Lane 3, *M.pg* treated with heat at 90°C; Lane 4, *M.pg* treated with heat at 100°C; Lane 5, *M.pg* treated with 4% formalin; Lane 6, *M.pg* treated with 70% ethanol. Molecular weight markers (kDa) are shown in the ladder lane.

injected with BCG Tokyo (5×10^5 cfu/mice) and 10 weeks later received either one (BCG+Inactivated Mpg^{1st}) or two (BCG+Inactivated Mpg^{2nd}) applications of an Inactive *M.pg* MAP (1×10^6 cells/patch) at 2-week intervals, or a single (BCG+Live Mpg^{1st}) application of a Live *M.pg* MAP (1×10^6 cells/patch).

Immunoassay in mice

To analyze the immune response, mice were euthanized either 4 weeks after the final vaccination, or at 6 weeks post-challenge. Cells isolated from the lungs and spleens were stimulated with H37Ra lysate and *M.pg* culture filtrate protein (CFP) for 12 or 24 hours. Subsequently, cells and supernatants were harvested, and flow cytometry and ELISA were performed to assess immune responses.

Challenge and bacterial enumeration in mice

To evaluate the vaccine efficacy, mice were infected with Mycobacterium tuberculosis (Mtb) H37Rv 4 weeks after the final vaccination. Briefly, following anesthetization with 1.2% 2,2,2-tribromoethanol (Avertin; Sigma), a small midline incision was made to expose the trachea, and each mice was intratracheally inoculated with 1×10^3 cfu/50uL of Mtb H37Rv. Intratracheal Mtb infections were conducted in a Class II B2 type Biological Safety Cabinet (ESCO, Seoul, Korea).

Mice were euthanized with CO_2 at 6 weeks post-challenge. Then, lungs and spleens were homogenized. The number of viable bacteria was determined by plating serial dilutions of the organ homogenates onto Middlebrook 7H10 agar (Difco, USA) supplemented 10% OADC (Difco, USA) and amphotericin B (Sigma Aldrich, USA). Colonies were counted after 4 weeks of incubation at 37°C. Protective efficacies were expressed as the log10-transformed bacterial count in immunized mice and were compared to the bacterial counts in the infection controls.

Enzyme-linked immunosorbent assay (ELISA)

Single-cell (1×10^6 cell/well) suspensions from lungs and spleens of mice were seeded in 96-well plates. Each group of cells was then stimulated with H37Ra lysate (5 μg/mL) and Mpg CFP (5 μg/mL) for 24 hours at 37°C in an incubator. Subsequently, Supernatant was harvested, and ELISA was performed to analyze cytokine levels. A sandwich ELISA was used to detect TNF-α (Invitrogen), IL-2 (Invitrogen), IL-17 (Thermo Fisher Scientific), and IFN-γ (Thermo Fisher Scientific) levels in culture supernatants as previously described [PMID: 21993523].

Flow cytometry

To generate single-cell suspensions, harvested lung and spleen tissue were incubated in RPMI digestion medium following a previously described protocol [PMID: 30849108]. Single-cell suspensions from each organ of immunized mice were stimulated with H37Ra lysate (5 μg/mL) or Mpg CFP (5 μg/mL) for 12 hours at 37°C in the presence of GogiStop (BD Biosciences) according to a previously described procedure [PMID: 30849108]. The cells were first blocked with Fc Block (eBioscience) for 15 min at 4°C and then stained with fluorophore-conjugated antibodies (Live/Dead, anti-90.2 (Thermo Fisher Scientific), anti-CD4, anti-CD8 (BD Biosciences)). Cells stained with isotype-matched immunoglobulins were used as negative controls. The cells were fixed and permeabilized using a Cytofix/Cytoperm (BD Biosciences) according to the manufacturer's instructions. Intracellular staining was performed in permeation buffer using fluorochrome-conjugated flow cytometry antibodies (IFN-γ, TNF-α,IL-2; BD Biosciences). Samples were subsequently analyzed using the NovoCyte flow cytometer and NovoCyte software.

Statistical analysis

All experiments were performed using GraphPad Prism 10 software (GraphPad software, San Diego, CA, USA). Statistical significance between groups was evaluated using one-way ANOVA followed by Fisher's multiple comparison test.

Results

Optimization of M. paragordonae inactivation for MAP vaccine production

The efficacy of inactivation treatments was assessed by counting colonies from 7H10-OADC agar plates and using a bacterial cell counter (QUANTOM Tx™, Logos Biosystems, South Korea). Heat (80, 90, and 100°C), formalin, and ethanol achieved 100% inactivation efficacy, with no bacterial growth observed on the plates or by cell counting. We applied complementary methods to evaluate the effects of the various inactivation treatments on the cellular morphology of inactivated M.pg.

Figure 1(a-f) shows SEM micrographs that confirm the maintenance of M.pg cellular morphology following the inactivation procedures. SEM micrographs revealed distinct structural alterations across treatment modalities. Untreated M.pg exhibited intact spherical structures with smooth surfaces ($1.28 \pm 0.15 \, \mu m$ diameter) 1, while thermal treatment induced progressive deformation – 80°C caused minor membrane wrinkling (Figure 1b), 90°C led to partial collapse (Figure 1c), and 100°C resulted in complete structural disintegration (Figure 1d). Chemical inactivation with 4% formalin preserved gross morphology but created surface nanopores ($38.6 \pm 12.4 \, nm$ diameter, Figure 1e) 1, whereas 70% ethanol treatment caused partial membrane fragmentation into <200 nm vesicles while maintaining particulate structure (Figure 1f). As the temperature of the heat treatment increases, the cellular morphology of M.pg appears to be progressively disrupted, with cells becoming distorted and clumping together. In contrast, formalin and ethanol treatments maintained well-preserved cellular morphology.

The stability of the Rv1886 (Ag85B) protein in M.pg following inactivation treatments was assessed using Western blot analysis (Figure 1g) using anti-Ag85B. Western blot analysis demonstrated treatment-specific protein degradation patterns. Thermal treatments above 80°C caused complete protein denaturation (Lanes 2–4, Figure 1g), while formalin treatment degraded whole protein (Lane 5). Ethanol treatment uniquely maintained the full spectrum of native protein bands (45–150 kDa range, Lane 6). All inactivation methods examined, except for ethanol treatment, resulted in a reduction of Ag85B levels relative to untreated M.pg. Ethanol-treated samples maintained Ag85B levels comparable to those observed in untreated M.pg. Inactivated MAP vaccine was fabricated with 1×10^6 CFU/MAP using ethanol-treated M.pg.

Immunogenicity comparison of live and inactivated M. paragordonae MAP vaccines

The results demonstrate that repeated administration of inactivated M.pg significantly enhances both CD4$^+$ and CD8$^+$ T cell responses in the spleen compared to single administration or live M.pg (Figure 2). Specifically, the second administration of inactivated M.pg (orange bars) elicited a marked increase in triple cytokine-producing T cells (IFN-γ/IL-2/TNF) and dual cytokine-producing populations (IFN-γ/IL-2, IFN-γ/TNF) for both antigen preparations (H37Ra lysate and Mpg CFP). H37Ra lysate consistently induced stronger cytokine responses than Mpg CFP across all conditions. Single IL-2 production was modestly increased only in CD8$^+$ T cells of the inactivated M.pg second administration group compared to other groups, while triple- and dual-cytokine (IFN/IL2/TNF, IFN/IL2) producing T cells were significantly elevated in the inactivated M.pg 2nd group.

Following in vitro stimulation with live or inactivated M.pg, the production of key pro-inflammatory cytokines IFN-gamma and TNF-alpha was significantly increased in both CD4$^+$ and CD8$^+$ T cell populations relative to naive controls ($p < .05$). Notably, the IL-2 response did not exhibit a similar significant increase compared to the naive group under these stimulation conditions. These findings suggest that repeated exposure to inactivated M.pg antigens effectively enhances specific cellular immune responses, particularly IFN-gamma and TNF-alpha production by both helper (CD4$^+$) and cytotoxic (CD8$^+$) T cells, which holds potential implications for vaccine strategies targeting intracellular pathogens. These findings indicate that repeated exposure to inactivated antigens boosts the immunogenicity of both helper (CD4$^+$) and cytotoxic (CD8$^+$) T cells, highlighting potential avenues for vaccine strategies. Correspondingly, our results confirmed the vaccine potential of Mpg, established foundational data informing challenge study design, and led to the planning of experiments applying these principles.

M. paragordonae booster augments BCG vaccine-induced protective CD4$^+$ and CD8$^+$ T cell responses

At 6 weeks post challenge (wpc), analysis of splenocytes (Figure 3a) revealed that the BCG+Live Mpg[1st] group exhibited significantly enhanced polyfunctional CD4$^+$ T cell responses. Specifically, this group showed markedly higher frequencies of CD4$^+$ T cells co-expressing IFN-γ, IL-2, and TNF-α (IFN/IL2/TNF) compared to both the naive and BCG-only groups upon stimulation with either H37Ra lysate or Mpg CFP. Furthermore, the BCG+Live Mpg[1st] group also demonstrated increased proportions of IFN-γ/IL-2 and TNF-α/IL-2 co-expressing CD4$^+$ T cell subsets, particularly after Mpg CFP stimulation. Consistent with this, the BCG+Inactivated M.pg groups also elicited strong immune responses. Notably, two administrations of inactivated M.pg (BCG+Inactivated Mpg[2nd]) resulted in significantly elevated levels of IL-2 and TNF-α production in CD4$^+$ T cells compared to a single administration (BCG+Inactivated Mpg[1st]). The BCG+Inactivated Mpg[2nd] group also showed a prominent increase in polyfunctional CD4$^+$ T cells producing IFN/IL2/TNF and
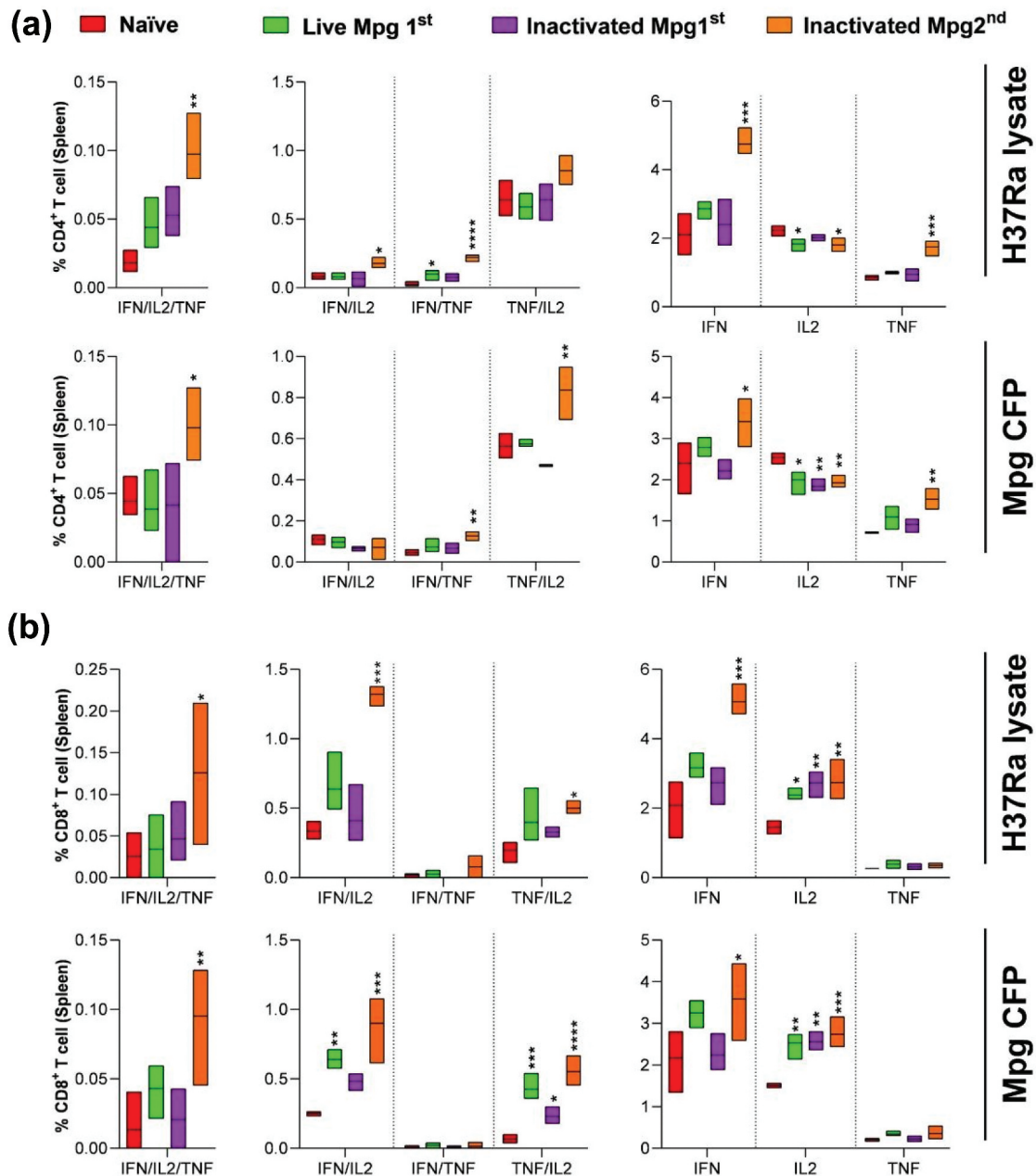
Figure 2. Analysis of cytokine production by CD4+ and CD8+ T cells in the spleen following stimulation with H37Ra lysate or Mpg CFP under different conditions. (a Percentages of CD4+ T cells producing triple (IFN-γ/IL-2/TNF), dual (IFN-γ/IL-2, IFN-γ/TNF, TNF/IL-2), or single (IFN-γ, IL-2, TNF) cytokines in response to stimulation with H37Ra lysate (top row) or Mpg CFP (bottom row). (b) Percentages of CD8+ T cells producing triple, dual, or single cytokines under the same conditions as in (a). The experimental groups include naïve (red), live Mpg[1st] administration (green), inactivated Mpg[1st] administration (purple), and inactivated Mpg[2nd] administration (orange). Data are presented as box plots showing the median and interquartile ranges, $n = 5$/group. Asterisks indicate statistical significance compared to the naive group, where $*p < .05$, $**p < .01$, $***p < .001$ and $****p < .0001$.

TNF/IL2, suggesting a dose-dependent boosting effect of inactivated *M.pg*. Conversely, the naive and BCG-only groups displayed minimal cytokine production across all cytokine subsets examined.

In the lung (Figure 3b) at 6 wpc, similar trends were evident. The BCG+Live *M.pg* group induced significantly higher frequencies of polyfunctional IFN/IL2/TNF-expressing CD4+ T cells compared to control groups, most notably upon Mpg CFP stimulation. Mirroring splenic responses, BCG +Inactivated Mpg[2nd] elicited superior responses compared to BCG+Inactivated Mpg[1st] in the lung, with significantly increased IL-2 and TNF-α production across multiple cytokine

subsets. In particular, the BCG+Inactivated Mpg[2nd] regimen induced robust IFN/IL2/TNF and TNF/IL2 co-expression in CD4+ T cells following stimulation with both H37Ra lysate and Mpg CFP. Importantly, at 0 wpc, no significant inter-group differences in cytokine production were detected in either spleen or lung, confirming that the observed enhanced cytokine responses at 6 wpc were attributable to post-challenge adaptive immunity and the applied vaccination strategies.

The data presented in Figure 4 demonstrates the cytokine production profiles of CD8+ T cells in both spleen (A) and lung (B) tissues at 0 and 6 weeks post-challenge (wpc) across different vaccination groups. At 0 pwc, BCG
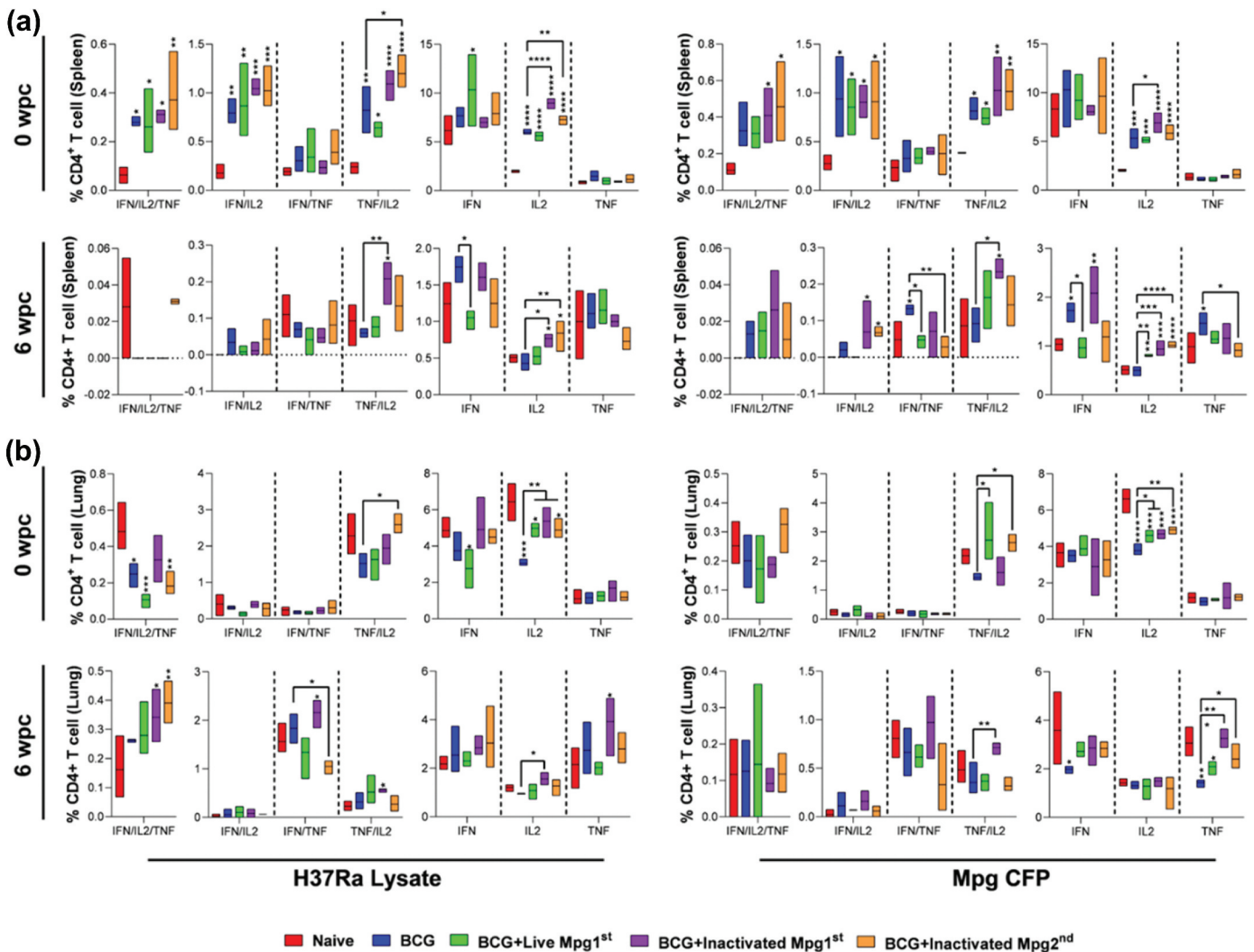
(a)

(b)

H37Ra Lysate   Mpg CFP

■ Naive ■ BCG ■ BCG+Live Mpg1st ■ BCG+Inactivated Mpg1st ■ BCG+Inactivated Mpg2nd

Figure 3. Polyfunctional CD4+ T cell responses in the spleen and lung following different vaccination regimens at 0 and 6 weeks post-challenge (wpc). (a) Frequencies of CD4+ T cells expressing combinations of IFN-γ, IL-2, and TNF-α (IFN/IL2/TNF, IFN/IL2, IFN/TNF, TNF/IL2) or single cytokines (IFN-γ, IL-2, TNF-α) in the spleen after stimulation with H37Ra lysate or Mpg CFP. (b) Frequencies of CD4+ T cells expressing the same cytokine combinations in the lung under identical stimulation conditions. Groups include naïve (red), BCG-only (green), BCG+Live Mpg1st (blue), BCG+Inactivated Mpg1st (once injection, purple), and BCG+Inactivated Mpg2nd (twice injections, orange). Data are presented as box plots showing median values (black line in bar) and interquartile ranges (bar), $n = 5$/group. Asterisks indicate statistical significance compared to the naive group, where *$p < .05$, **$p < .01$, ***$p < .001$ and ****$p < .0001$.

vaccination alone and in combination with various *M.pg* formulations induced polyfunctional CD8+ T cells producing IFN/IL2, with significant differences observed compared to the naïve group, particularly in lung tissue. The H37Ra lysate stimulation showed stronger IFN responses in the BCG and BCG+Live Mpg1st groups. At 6 pwc, the cytokine profiles shifted, with notable increases in IFN/TNF producing cells in the spleen for the BCG +Inactivated Mpg1st group when stimulated with Mpg CFP. In the lung, BCG vaccination maintained robust CD8+ T cell responses across multiple cytokine combinations. The BCG+Inactivated Mpg2nd group demonstrated enhanced TNF/IL2 responses in the lung when stimulated with H37Ra lysate. These results indicate that BCG vaccination, particularly when boosted with inactivated *M.pg* formulations, promotes durable and polyfunctional CD8+ T cell responses that may contribute to enhanced protection against mycobacterial challenge.

Induction of memory T cell responses following BCG and *M. paragordonae* booster vaccination

The results demonstrate the differential induction of central memory (T_{cm}) and effector memory (T_{em}) T cell subsets in CD4+ and CD8+ T cells following various vaccination regimens at 0 and 6 weeks post-challenge (wpc). For CD4+ T cells (Figure 5a), the percentage of T_{em} cells was significantly higher in the BCG+Live Mpg1st and BCG+Inactivated Mpg1st groups compared to the naive and BCG-only groups in response to both H37Ra lysate and Mpg CFP stimulation at 0 wpc. At 6 wpc, this trend persisted, with BCG+Live Mpg1st showing the highest T_{em} cell induction. However, no significant differences were observed in CD4+ T_{cm} populations across groups at either time point. For CD8+ T cells (Figure 5b), a similar pattern was observed, with BCG+Live Mpg1st and BCG+Inactivated Mpg1st inducing significantly higher percentages of T_{em} cells compared to controls at 0 wpc, particularly in response to Mpg CFP stimulation. At 6 wpc, the BCG+Inactivated Mpg2nd group
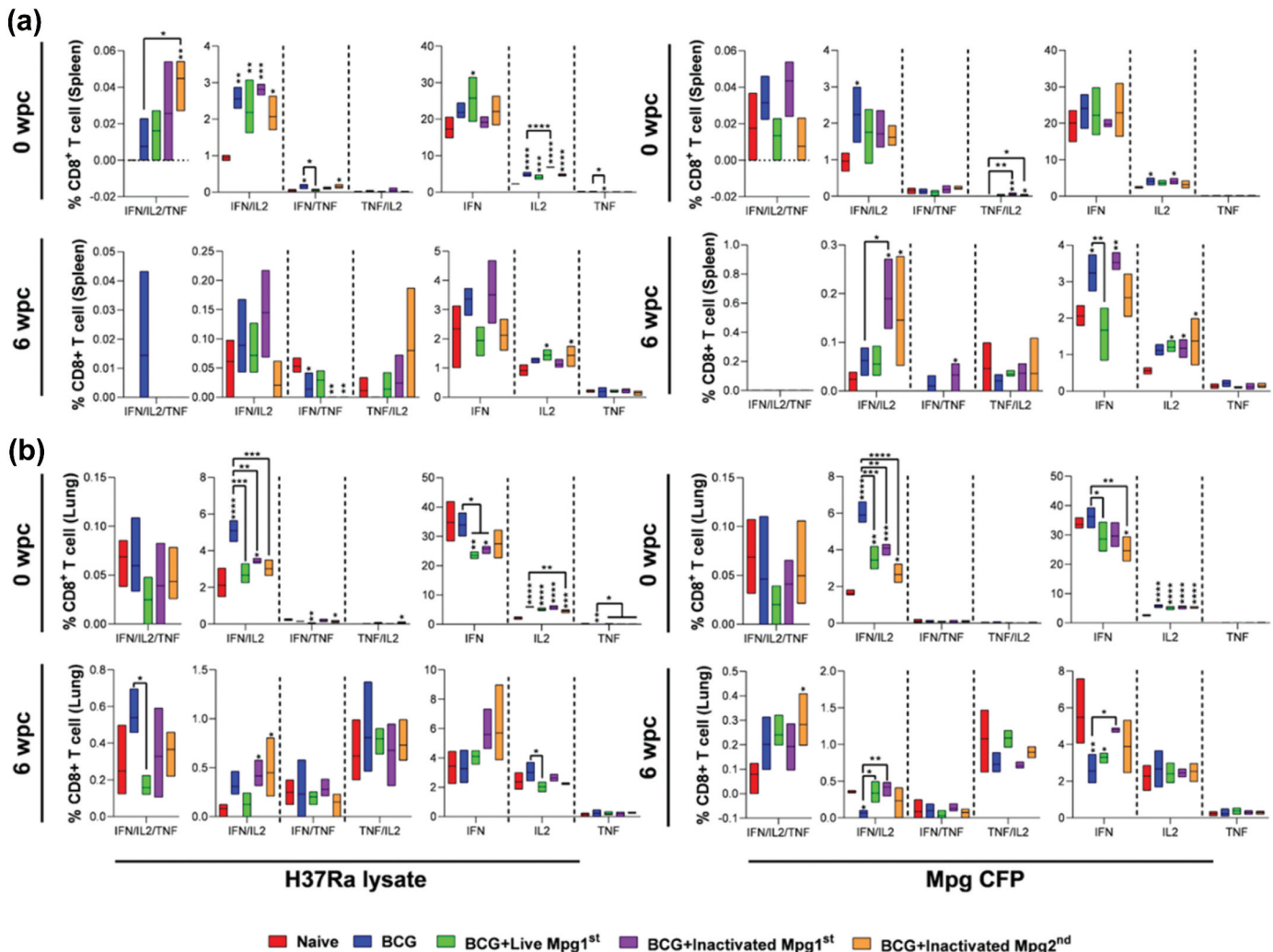
Figure 4. Polyfunctional CD8$^+$ T cell responses in the spleen and lung following different vaccination regimens at 0 and 6 weeks post-challenge (wpc). (a) Frequencies of CD8$^+$ T cells expressing combinations of IFN-γ, IL-2, and TNF-α (IFN/IL2/TNF, IFN/IL2, IFN/TNF, TNF/IL2) or single cytokines (IFN-γ, IL-2, TNF-α) in the spleen after stimulation with H37Ra lysate or mpg CFP. (b) Frequencies of CD8$^+$ T cells expressing the same cytokine combinations in the lung under identical stimulation conditions. Groups include naive (red), BCG-only (green), BCG+Live Mpg^{1st} (blue), BCG+Inactivated Mpg^{1st} (once injection, purple), and BCG+Inactivated Mpg^{2nd} (twice injections, orange). Data are presented as box plots showing median values (black line in bar) and interquartile ranges (bar), $n = 5$/group. Asterisks indicate statistical significance compared to the naive group, where *$p < .05$, **$p < .01$, ***$p < .001$ and ****$p < .0001$.

exhibited a notable increase in CD8$^+$ T$_{em}$ cells. Interestingly, CD8$^+$ T$_{cm}$ populations were generally low across all groups, with only modest increases observed in the BCG+Live Mpg^{1st} group at 0 wpc. These findings suggest that co-administration of live or inactivated *M.pg* enhances the generation of antigen-specific effector memory T cells, particularly in response to mycobacterial antigens, indicating a potential strategy for improving vaccine efficacy against mycobacterial infections.

Enhanced cytokine production in pulmonary and splenic tissues following BCG-M. paragordonae vaccination

Analysis of cytokine production in lung (Figure 6a) and spleen (Figure 6b) tissues revealed distinct responses across vaccination groups and time points. At 6 weeks post-challenge (wpc), BCG vaccination, particularly in combination with *M.pg* boosters, significantly enhanced cytokine production compared to the naive group.

In the lung, BCG+Live Mpg^{1st} and BCG+Inactivated Mpg^{2nd} groups demonstrated markedly elevated levels of IFN-γ and TNF-α production, particularly upon H37Ra lysate stimulation (*$p < .001$ and *$p < .01$, respectively for IFN-γ; **$p < .001$ for TNF-α in both groups). While IL-2 production showed a significant increase in BCG+Live Mpg^{1st} with H37Ra lysate stimulation ($p < .05$), IL-17 production remained largely unchanged across groups and stimuli in the lung.

In the spleen, a more pronounced and broad cytokine response was observed. Both BCG+Live Mpg^{1st} and BCG+Inactivated Mpg^{2nd} groups exhibited significant increases in IFN-γ, TNF-α, and IL-2 production following H37Ra lysate stimulation (*$p < .001$, ****$p < .0001$, and **$p < .01$ respectively for IFN-γ in both groups; ****$p < .0001$ and ***$p < .001$, and **$p < .01$ for TNF-α; **$p < .01$ and **$p < .01$, and $p < .05$ for IL-2). Notably, IFN-γ and TNF-α production in the spleen of

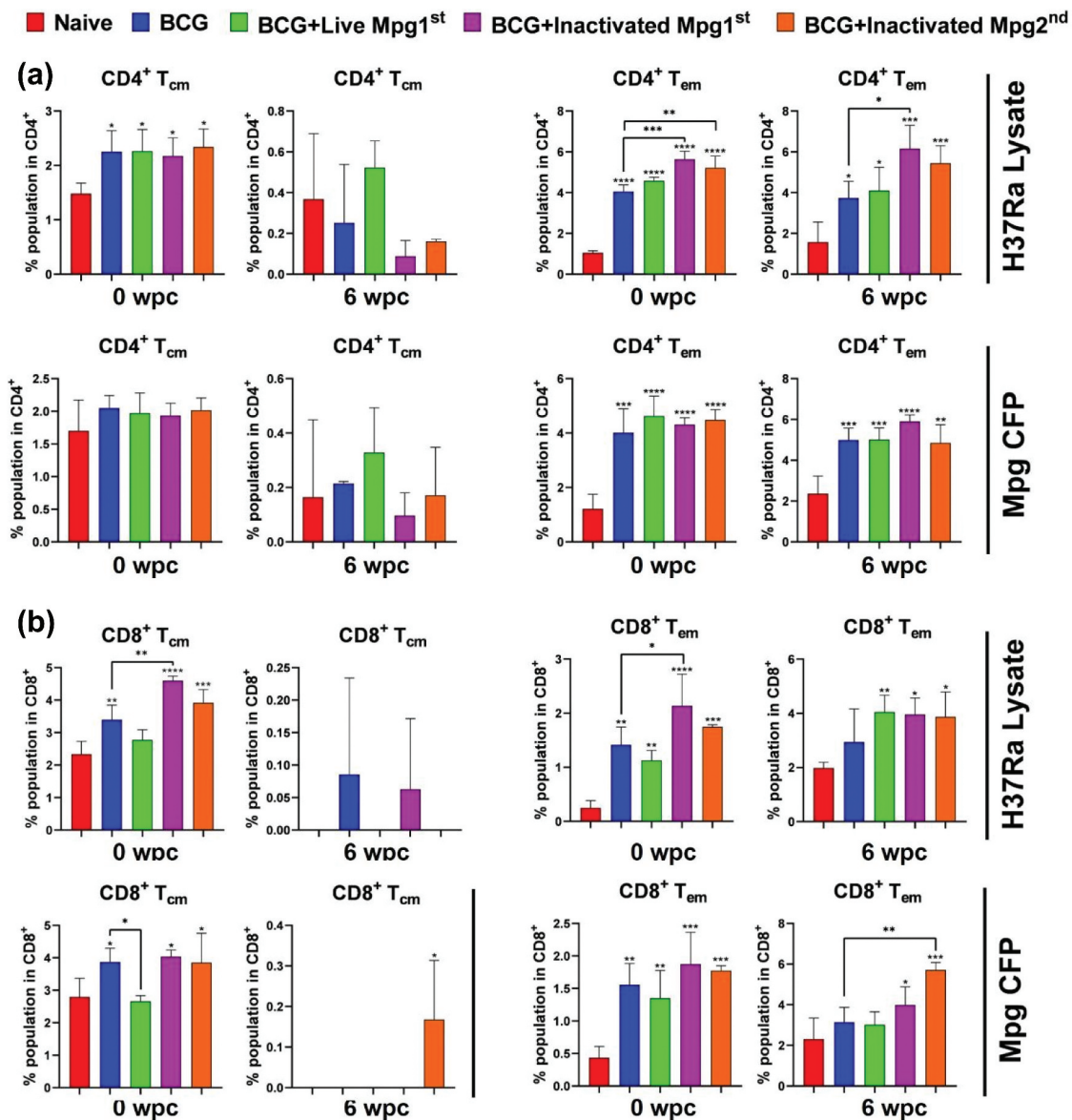**Figure 5.** Memory CD4+ and CD8+ T cell responses in Spleen and lung following BCG vaccination and M.Pg Boosting. (a) Spleen and (b) lung cells stimulated with H37Ra lysate or Mpg CFP were analyzed for the percentage of central memory T cells (Tcm) and effector memory T cells (Tem) within CD4+ and CD8+ T cell populations. Graphs depict the percentages at 0 weeks post-challenge (0 wpc) and 6 weeks post-challenge (6 wpc) for each treatment group: naive, BCG, BCG+Live Mpg1st, BCG+Inactivated Mpg1st, and BCG+Inactivated Mpg2nd. Data in bar graphs are presented as mean ± SD. Asterisks indicate statistical significance compared to the naive group, where $*p < .05$, $**p < .01$, $***p < .001$ and $****p < .0001$.

BCG+Live Mpg^{1st} and BCG+Inactivated Mpg^{2nd} groups reached considerably higher levels than in other groups.

With Mpg CFP stimulation, cytokine production was generally lower compared to H37Ra lysate, but BCG+Live Mpg^{1st} and BCG+Inactivated Mpg^{2nd} groups still maintained elevated levels of IFN-γ and TNF-α in both lung and spleen, with significant increases observed for IFN-γ in the lung of BCG+Live Mpg^{1st} and BCG+Inactivated Mpg^{2nd} groups ($*p < .05$ and $p < .05$, respectively) and for TNF-α in the lung of BCG+Inactivated Mpg^{2nd} ($p < .05$). At 0 wpc, cytokine production was minimal, and no significant differences were observed across groups in either tissue, indicating that the enhanced cytokine responses at 6 wpc were driven by vaccination and booster strategies post-challenge.

Protective efficacy against M. tuberculosis *H37Rv* infection

Six-weeks following intratracheal *M. tuberculosis* H37Rv infection, a cohort of five mice per group were assessed for bacterial burden within the lung and spleen as the primary endpoints for protective efficacy (Figure 7). The bacterial burden in both the lungs and spleen was significantly reduced in all vaccinated groups compared to the naïve group (G1) following the challenge test. In the lungs (left panel), the BCG-only group (G2) exhibited a marked reduction in bacterial CFU counts compared to G1 (**, $p < .0001$). Furthermore, co-administration of BCG with *M.pg* as a booster vaccine (G3-G5) resulted in an even greater reduction in bacterial loads. Among these, G5 demonstrated the lowest bacterial burden, indicating enhanced protective efficacy. Similarly, in the spleen (right panel), all
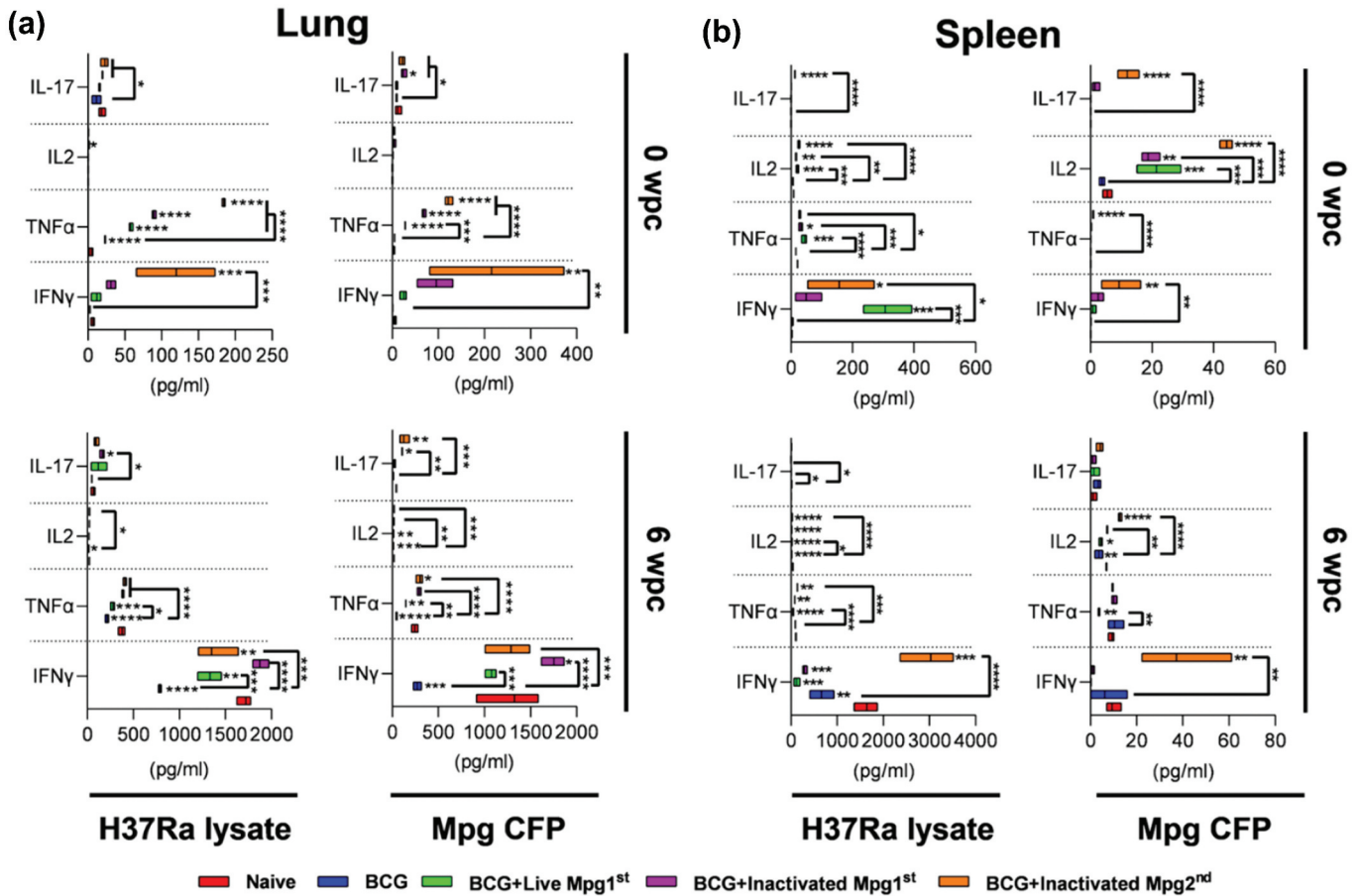
Figure 6. Cytokine production in lung and spleen tissues following vaccination and booster strategies. Panels (a) and (b) illustrate cytokine levels in lung and spleen tissues, respectively, at 0 and 6 weeks post-challenge (wpc). Cytokine production of IL-17, IL-2, TNF-α, and IFN-γ (pg/ml) are presented for each group (naive, BCG, BCG +Live Mpg[1st], BCG+Inactivated Mpg[1st], BCG+Inactivated Mpg[2nd]). Box plots represent cytokine concentrations for each group, with the horizontal line within the box indicating the median, the box range representing the interquartile range, and whiskers representing the data range. The upper panels show cytokine production following in vitro restimulation with H37Ra lysate, while the lower panels show cytokine production following in vitro restimulation with Mpg CFP. Statistical significance was determined using one-way ANOVA followed by Fisher's multiple comparisons test. Data are presented as box plots showing median values (black line in bar) and interquartile ranges (bar), $n = 5$/group. Asterisks indicate statistical significance compared to the naive group, where $*p < .05$, $**p < .01$, $***p < .001$ and $****p < .0001$.
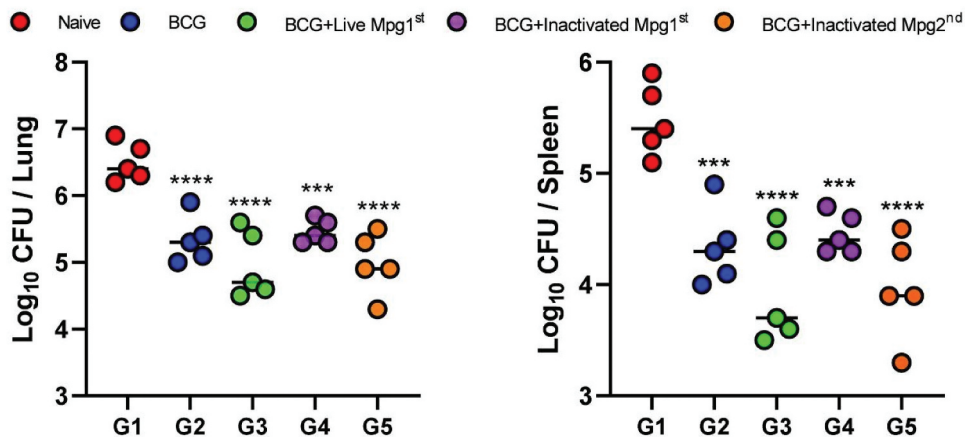

Figure 7. All prime/boost vaccine strategies provide prophylactic pulmonary protection against *M. tuberculosis* H37Rv in mice. mice were infected with *M. tuberculosis* H37Rv by intratracheal route four or six weeks post final immunization. (a, b) bacterial burden was assessed by colony forming unit (CFU) in lung (a) and spleen (b) organ homogenates six weeks post challenge. CFU means were compared between each group using one-way ANOVA with Fisher's multiple comparisons test. The Black line showed mean, dots represent individual mice, $n = 5$/group. Asterisks indicate statistical significance compared to the naive group, where $*p < .05$, $**p < .01$, $***p < .001$ and $****p < .0001$.

vaccinated groups showed significantly lower CFU counts compared to G1. The BCG-only group (G2) provided significant protection (*, $p < .001$), while the use of *M.pg* as a booster vaccine (G3-G5) further improved outcome. Notably, G5 again showed the most pronounced reduction in bacterial dissemination to the spleen. These results suggest that *M.pg*, particularly in its inactivated form administered as a second booster, significantly enhances the protective effect of BCG vaccination against systemic bacterial dissemination during challenge tests.

Discussion

The development of effective *tuberculosis* (TB) vaccines remains an urgent global health priority, particularly given the limitations of the century-old Bacillus Calmette-Guérin (BCG) vaccine and the rising TB incidence worldwide. Persistent high TB cases highlight the BCG vaccine's limited long-term protection, especially in adults, driving research into boosters like *nontuberculous mycobacteria* (NTM). In this study, we developed and evaluated an inactivated *Mycobacterium paragordonae* (*M.pg*) microneedle array patch (MAP) vaccine as a novel booster candidate to enhance the efficacy of the Bacillus Calmette-Guérin (BCG) vaccine against TB.

The results demonstrate that ethanol-inactivated *M.pg* maintains cellular morphology and protein integrity while achieving complete bacterial inactivation, making it an ideal candidate for vaccine development. Importantly, the ethanol treatment uniquely preserved the full spectrum of native protein bands in the 45–150 kDa range, including the immunologically significant Ag85B protein, which was degraded by other inactivation methods (Figure 1). Whole-cell killed bacterial vaccines present a safe and broadly applicable vaccination strategy due to their preservation of key bacterial antigens, which elicit robust antigenicity and offer comprehensive serotype coverage. Furthermore, their potential for cost-effective and straightforward preparation and administration renders them particularly relevant for resource-limited settings. Taddese *et al.* (2021) showed that BPL, ethanol and formalin treatments generated inactivated bacteria with preserved cellular integrity.[27] Indeed, the protective efficacy of whole-cell killed pneumococcal vaccines[28,29] and Vibrio proteolyticus[30,31] using ethanol treatment has been substantiated. The choice of ethanol as an inactivating agent also addresses safety concerns associated with live attenuated vaccines. The inability of inactivated pathogens to revert to virulence is a critical safety advantage. Live attenuated vaccines, such as BCG for TB, carry risks of adverse events in immunocompromised individuals.[32] In contrast, *Salmonella Enteritidis* inactivated vaccines caused no systemic reactions in chickens, even at high doses, validating their safety.[33] This aliLgns with global preferences for inactivated platforms in high-risk populations, including immunocompromised patients.[34] While live *M.pg* MAPs previously showed efficacy, their potential for reactivation or unintended persistence in immunocompromised hosts necessitates caution. Ethanol inactivation eliminates these risks while preserving immunogenicity, mirroring the success of DAR-901 (inactivated *M. obuense*).[35]

MAP has emerged as a promising transdermal immunization strategy.[36–38] While several microneedle systems have been approved or investigated clinically, most dissolving-type microneedles are fabricated using a complex, multi-step molding process involving harsh curing conditions.[39,40] This limits their suitability for heat-sensitive biological drugs. The DEN method offers a simpler, more efficient approach, enabling drug loading without loss and precise dose control. By eliminating the need for mold, the DEN method facilitates mass production and reduces fabrication costs. This method's compatibility with heat-sensitive drugs, such as vaccines, further enhances its market competitiveness. The skin's rich immune environment, with abundant antigen-presenting cells in the epidermis and dermis, provides an ideal target for vaccine delivery. The MAP format facilitates efficient targeting of these immune cells, potentially enhancing vaccine immunogenicity compared to traditional injection routes.

Primary immunogenicity results utilizing the DEN microarray patch fabrication method revealed substantial potential for combining inactivated *M.pg* and MAP (Figure 2). We observed that inactivated *M.pg* MAP robustly enhanced cytokine expression, an effect consistently replicated in subsequent challenge tests. The prime-boost regimen, employing BCG priming followed by inactivated *M.pg* MAP boosting, elicited a potent Th1-polarized immune response, characterized by elevated production of IFN-γ, TNF-α, and IL-2 in both CD4$^+$ and CD8$^+$ T cell populations (Figures 3–4). Notably, two administrations of inactivated *M.pg* following BCG priming (BCG+Inactivated Mpg^{2nd}) proved particularly efficacious, inducing polyfunctional T cell populations that surpassed responses observed with BCG alone or live *M.pg* boosters. Furthermore, this BCG+Inactivated Mpg^{2nd} regimen successfully generated effector memory T cells (Tem) within both pulmonary and splenic tissues (Figure 5).

The exclusion of a BCG-BCG control group from this study design was a deliberate decision based on substantial clinical and epidemiological evidence. Extensive clinical trials, including a large-scale study with a 15-year follow-up period involving 4,436 participants, have demonstrated that BCG revaccination confers no significant additional protective efficacy against adult pulmonary tuberculosis compared to a single primary BCG vaccination.[41] This finding is further corroborated by the World Health Organization's (WHO) 1999 recommendation advising against routine BCG revaccination,[42] as well as recent data from a phase 3 clinical trial (NCT04152161) indicating only 45.4% efficacy of BCG revaccination against latent tuberculosis infection.[43] Consequently, our research focus on evaluating novel booster candidates aligns with the global scientific consensus and ongoing efforts to develop improved vaccination strategies that supersede the repetition of BCG administration, a practice now considered to possess limited clinical utility.

Lung-resident T$_{em}$ cells are critical for intercepting *M. tuberculosis* upon inhalation, and their induction here correlates with the significant reduction in pulmonary bacterial burden post-challenge (Figure 7a). The concomitant suppression of splenic dissemination (Figure 7b) further underscores systemic protection, likely mediated by

circulating memory T cells primed by MAP-delivered antigens. The trade-off between convenience and efficacy is evident in inactivated vaccine design. For example, inactivated Japanese encephalitis vaccines showed 96–100% seroconversion after two doses, mirroring live vaccine performance.[35] Similarly, M.pg's two-dose regimen increased cytokine by single dosing, highlighting the importance of booster schedules.

The immunogenicity of inactivated *M.pg* MAPs may arise from synergistic innate and adaptive activation. Ethanol-preserved pathogen-associated molecular patterns (PAMPs) such as lipoarabinomannan (LAM) and trehalose dimycolate (TDM) likely engage TLR2/4 and Mincle receptors on antigen-presenting cells.[44,45] This innate signaling potentiates dendritic cell maturation and migration to lymph nodes, where they prime naïve T cells.[46] The robust CD8+ T cell responses observed (Figure 4) suggest cross-presentation of antigens via MHC-I, a process enhanced by MAPs' intradermal delivery.

Surprisingly, IL-17 production remained unchanged across groups (Figure 6). While Th17 responses contribute to mucosal immunity, their absence here implies that the BCG/*M.pg* booster primarily strengthens Th1 pathways.[47,48] This aligns with murine models where IFN-γ and TNF-α dominate protection against TB. Additionally, IL-17 production remained low across all vaccination groups, which is consistent with the known Th17 response profile of C57BL/6 mice.[49] As this strain is genetically predisposed to attenuated IL-17 responses, future studies using BALB/c mice or humanized models will be important to fully evaluate the potential of M.pg MAP vaccination to induce Th17-mediated mucosal immunity. However, human translation may require balancing Th1/Th17 responses to avoid immunopathology, warranting cytokine profiling in non-human primates.[12,50,51] These cytokines are widely recognized as critical mediators for effective anti-mycobacterial immunity. Indeed, IFN-γ is a cornerstone cytokine for controlling mycobacterial infections by activating macrophages and promoting Th1 differentiation, while IL-2 is essential for T cell proliferation and survival and TNF-α contributes to granuloma formation and bacterial clearance.[52–55] In this study, our findings establish inactivated *M.pg* delivered via MAP as an effective booster strategy for enhancing BCG-induced protection against tuberculosis, with a two-dose schedule demonstrating optimal efficacy.

This approach combines the safety advantages of an inactivated vaccine with the practical benefits of microneedle delivery, addressing key limitations of current *tuberculosis* vaccination strategies. Although no adverse reactions or toxicity were observed throughout our study, comprehensive safety assessments remain essential before advancing to clinical applications.

In future research, we plan to conduct extensive toxicity studies to thoroughly evaluate the safety profile of inactivated *M.pg* delivered via microneedle patches. These studies will include acute and chronic toxicity assessments, local reactogenicity, and systemic biocompatibility analyses to ensure the vaccine's safety for potential human use. Future studies will focus on comprehensive safety evaluations, optimization of dosing intervals, and assessment of long-term protection to further develop this promising vaccine candidate.

Conclusion

In conclusion, our research establishes ethanol-inactivated *M.pg* delivered via microneedle array patches as a promising tuberculosis vaccine candidate. This method uniquely preserves cellular morphology and maintains the integrity of immunologically significant proteins, particularly Ag85B, likely contributing to the robust immunogenicity observed.

The immunological data provides compelling evidence for the efficacy of the inactivated *M.pg* MAP vaccine as a BCG booster, with two administrations significantly enhancing protective immune responses characterized by elevated IFN-γ, TNF-α, and IL-2 production in both CD4+ and CD8+ T cells. This polyfunctional T cell response is crucial for protection against mycobacterial infections. The strategy effectively generates effector memory T cells in both lung and spleen tissues, contributing to the significant reduction in bacterial burden observed in our challenge studies. The BCG+Inactivated M.pg[2nd] group consistently demonstrated the greatest reduction in bacterial burden in both organs.

The microneedle array patch delivery system offers practical advantages over conventional vaccination methods in resource-limited settings with high *tuberculosis* burden. Future research should focus on toxicity studies, optimization of dosing intervals, and assessment of long-term protection. The absence of significant IL-17 production suggests our formulation primarily strengthens Th1 pathways rather than Th17-mediated immunity, an area for future investigation.

Inactivated *M.pg* delivered via microneedle patches represents an effective booster strategy for enhancing BCG-induced protection against tuberculosis, with a two-dose schedule demonstrating optimal efficacy. This approach combines safety advantages with practical benefits, addressing key limitations of current vaccination strategies.

Author contributions

CRediT: **Moonsu Lee:** Formal analysis, Funding acquisition, Investigation, Methodology, Project administration, Writing – original draft; **Dohyeon Jeong:** Conceptualization, Supervision; **Kiyoung Yoon:** Data curation, Investigation, Methodology, Software, Visualization; **Juyoung Jin:** Funding acquisition, Project administration; **Yong Woo Back:** Data curation, Software; **In-Taek Jang:** Investigation; **Hwa-Jung Kim:** Methodology; **Bum-Joon Kim:** Resources; **Sung Min Bae:** Conceptualization, Formal analysis, Investigation, Methodology, Writing – review & editing.

Funding

Notes on contributor

Sung Min Bae, A highly motivated professional with approximately 10 years of experience in the vaccine development industry. My expertise lies in recombinant protein expression, with a strong focus on utilizing the baculovirus expression vector system. Throughout my career, I have been deeply involved in the development process of various vaccines. I am passionate about contributing to advancements in healthcare through innovative research and development in the field of vaccine technology.

Data available statement

The data that support the findings of this study are available from the corresponding author, Sung Min Bae, upon reasonable request.

References

1. World Health Organization. Global tuberculosis report 2024. 1st ed. Geneva: World Health Organization; 2024.
2. Lange C, Aaby P, Behr MA, Donald PR, Kaufmann SHE, Netea MG, Mandalakas AM. 100 years of Mycobacterium Bovis Bacille Calmette-Guérin. Lancet Infect Dis. 2022;22(1):e2–e12. doi: 10.1016/S1473-3099(21)00403-5.
3. Fine PEM, Carneiro IAM, Milstien JB, Clements CJ, Organization WH. Issues relating to the use of BCG in immunization programmes: a discussion document; 1999 [accessed 2025 Mar 4]. https://iris.who.int/handle/10665/66120.
4. Martinez L, Cords O, Liu Q, Acuna-Villaorduna C, Bonnet M, Fox GJ, Carvalho ACC, Chan P-C, Croda J, Hill PC, et al. Infant BCG vaccination and risk of pulmonary and extrapulmonary tuberculosis throughout the life course: a systematic review and individual participant data meta-analysis. Lancet Glob Health. 2022;10(9):e1307–e1316. doi: 10.1016/S2214-109X(22)00283-2.
5. Andersen P, Doherty TM. The success and failure of BCG - Implications for a novel tuberculosis vaccine. Nat Rev Microbiol. 2005;3(8):656–662. doi: 10.1038/nrmicro1211.
6. Nemes E, Geldenhuys H, Rozot V, Rutkowski KT, Ratangee F, Bilek N, Mabwe S, Makhethe L, Erasmus M, Toefy A, et al. C-040-404 Study Team. Prevention of M. Tuberculosis infection with H4: IC31 vaccine or BCG revaccination. N Engl J Med. 2018;379 (2):138–149. doi: 10.1056/NEJMoa1714021.
7. Treatment Action Group. 2022 pipeline report. [accessed 2025 Mar 4]. https://www.treatmentactiongroup.org/resources/pipeline-report/2022-pipeline-report/.
8. von Reyn CF, Lahey T, Arbeit R, Landry B, Kailani L, Adams L, Haynes B, Mackenzie T, Wieland-Alter W, Connor R, et al. Safety and immunogenicity of an inactivated whole cell tuberculosis vaccine booster in adults primed with BCG: a randomized, controlled trial of DAR-901. PLOS ONE. 2017;12(5):e0175215. doi: 10. 1371/journal.pone.0175215.
9. Poyntz HC, Stylianou E, Griffiths KL, Marsay L, Checkley AM, McShane H. Non-tuberculous mycobacteria have diverse effects on BCG efficacy against mycobacterium tuberculosis. Tuberc Edinb Scotl. 2014;94(3):226–237. doi: 10.1016/j.tube.2013.12.006.
10. Flaherty DK, Vesosky B, Beamer GL, Stromberg P, Turner J. Exposure to mycobacterium avium can modulate established immunity against mycobacterium tuberculosis infection generated by mycobacterium bovis BCG vaccination. J Leukoc Biol. 2006;80 (6):1262–1271. doi: 10.1189/jlb.0606407.
11. Kim B-J, Hong S-H, Kook Y-H, Kim B-J. Mycobacterium paragordonae Sp. Nov. a slowly growing, scotochromogenic species closely related to mycobacterium Gordonae. Int J Syst Evol Microbiol. 2014;64(Pt 1):39–45. doi: 10.1099/ijs.0.051540-0.
12. Kim B-J, Kim B-R, Kook Y-H, Kim B-J. A temperature sensitive mycobacterium paragordonae induces enhanced protective immune responses against mycobacterial infections in the mouse model. Sci Rep. 2017;7(1):15230. doi: 10.1038/s41598-017-15458-7.
13. Kim B-J, Kim B-R, Kook Y-H, Kim B-J. Potential of recombinant mycobacterium paragordonae expressing HIV-1 gag as a prime vaccine for HIV-1 infection. Sci Rep. 2019;9(1):15515. doi: 10. 1038/s41598-019-51875-6.
14. Kim B-J, Jeong H, Seo H, Lee M-H, Shin HM, Kim B-J. Recombinant mycobacterium paragordonae expressing SARS-CoV-2 receptor-binding domain as a vaccine candidate against SARS-CoV-2 infections. Front Immunol. 2021;12:712274. doi: 10.3389/fimmu.2021.712274.
15. Mishra R, Pramanick B, Maiti TK, Bhattacharyya TK. Glassy carbon microneedles—new transdermal drug delivery device derived from a scalable C-MEMS process. Microsyst Nanoeng. 2018;4(1):1–11. doi: 10.1038/s41378-018-0039-9.
16. Leone M, Priester MI, Romeijn S, Nejadnik MR, Mönkäre J, O'Mahony C, Jiskoot W, Kersten G, Bouwstra JA. Hyaluronan-based dissolving microneedles with high antigen content for intra-dermal vaccination: formulation, physicochemical characterization and immunogenicity assessment. Eur J Pharm Biopharm Off J Arbeitsgemeinschaft Pharm Verfahrenstech EV. 2019;134:49–59. doi: 10.1016/j.ejpb.2018.11.013.
17. Kim NW, Kim S-Y, Lee JE, Yin Y, Lee JH, Lim SY, Kim ES, Duong HTT, Kim HK, Kim S, et al. Enhanced cancer vaccination by in situ nanomicelle-generating dissolving microneedles. ACS Nano. 2018;12(10):9702–9713. doi: 10.1021/acsnano.8b04146.
18. Menon I, Bagwe P, Gomes KB, Bajaj L, Gala R, Uddin MN, D'Souza MJ, Zughaier SM. Microneedles: a new generation vaccine delivery system. Micromachines. 2021;12(4):435. doi: 10. 3390/mi12040435.
19. Zhang L, Guo R, Wang S, Yang X, Ling G, Zhang P. Fabrication, evaluation and applications of dissolving microneedles. Int J Pharm. 2021;604:120749. doi: 10.1016/j.ijpharm.2021. 120749.
20. Steinbach S, Jalili-Firoozinezhad S, Srinivasan S, Melo MB, Middleton S, Konold T, Coad M, Hammond PT, Irvine DJ, Vordermeier M, et al. Temporal dynamics of intradermal cytokine response to tuberculin in mycobacterium bovis BCG-Vaccinated cattle using sampling microneedles. Sci Rep. 2021;11(1). doi: 10. 1038/s41598-021-86398-6.
21. Jeong S-Y, Park J-H, Lee Y-S, Kim Y-S, Park J-Y, Kim S-Y. The current status of clinical research involving microneedles: a systematic review. Pharmaceutics. 2020;12(11):1113. doi: 10. 3390/pharmaceutics12111113.
22. Kim Y-C, Quan F-S, Compans RW, Kang S-M, Prausnitz MR. Formulation and coating of microneedles with inactivated influenza virus to improve vaccine stability and immunogenicity. J Control Release Off J Control Release Soc. 2010;142 (2):187–195. doi: 10.1016/j.jconrel.2009.10.013.
23. Tran KTM, Gavitt TD, Farrell NJ, Curry EJ, Mara AB, Patel A, Brown L, Kilpatrick S, Piotrowska R, Mishra N, et al. Transdermal microneedles for the programmable burst release of multiple vaccine payloads. Nat Biomed Eng. 2021;5(9):998–1007. doi: 10.1038/ s41551-020-00650-4.
24. Clayton K, Vallejo AF, Davies J, Sirvent S, Polak ME. Langerhans Cells-Programmed by the epidermis. Front Immunol. 2017;8:1676. doi: 10.3389/fimmu.2017.01676.
25. Chen Y-H, Lai K-Y, Chiu Y-H, Wu Y-W, Shiau A-L, Chen M-C. Implantable microneedles with an immune-boosting function for effective intradermal influenza vaccination. Acta Biomater. 2019;97:230–238. doi: 10.1016/j.actbio.2019.07.048.
26. Lee M-H, Seo H, Lee M-S, Kim BJ, Kim HL, Lee DH, Oh J, Shin JY, Jin JY, Jeong DH, et al. Protection against tuberculosis achieved by dissolving microneedle patches loaded with live mycobacterium

paragordonae in a BCG prime-boost strategy. Front Immunol. 2023;14:1178688. doi: 10.3389/fimmu.2023.1178688.

27. Taddese R, Belzer C, Aalvink S, de Jonge MI, Nagtegaal ID, Dutilh BE, Boleij A. Production of inactivated gram-positive and gram-negative species with preserved cellular morphology and integrity. J Microbiological Methods. 2021;184:106208. doi: 10.1016/j.mimet.2021.106208.

28. Hvalbye BK, Aaberge IS, Løvik M, Haneberg B. Intranasal immunization with heat-inactivated streptococcus pneumoniae protects mice against systemic pneumococcal infection. Infect Immun. 1999;67(9):4320–4325. doi: 10.1128/IAI.67.9.4320-4325.1999.

29. Lu Y-J, Yadav P, Clements JD, Forte S, Srivastava A, Thompson CM, Seid R, Look J, Alderson M, Tate A, et al. Options for inactivation, adjuvant, and route of topical administration of a killed, unencapsulated pneumococcal whole-cell vaccine. Clin Vaccine Immunol CVI. 2010;17(6):1005–1012. doi: 10.1128/CVI.00036-10.

30. García-Márquez J, Vizcaíno AJ, Barany A, Galafat A, Acién G, Figueroa FL, Alarcón FJ, Mancera JM, Martos-Sitcha JA, Arijo S, et al. Evaluation of the combined administration of chlorella fusca and Vibrio Proteolyticus in diets for Chelon Labrosus: effects on growth, metabolism, and digestive functionality. Animals. 2023;13(4):589. doi: 10.3390/ani13040589.

31. Medina A, García-Márquez J, Moriñigo MÁ, Arijo S. Effect of the potential probiotic vibrio proteolyticus DCF12.2 on the immune system of Solea Senegalensis and protection against photobacterium damselae Subsp. Piscicida and vibrio Harveyi. Fishes. 2023;8(7):344. doi: 10.3390/fishes8070344.

32. Kaufmann SHE. Vaccine development against tuberculosis over the last 140 years: failure as part of success. Front Microbiol. 2021;12:750124. doi: 10.3389/fmicb.2021.750124.

33. Kang ZW, Won H, Kim EH, Noh YH, Choi HW, Hahn TW. Protective effects and immunogenicity of salmonella enteritidis killed vaccine strains selected from virulent salmonella enteritidis isolates. Korean J Vet Res. 2011;51(1):21–28. doi: 10.14405/kjvr.2011.51.1.021.

34. Adduri S, Bohorquez JA, Adejare O, Rincon D, Tucker T, Konduru NV, Yi G. Spatial transcriptomic analysis of HIV and tuberculosis coinfection in a humanized mouse model reveals specific transcription patterns, immune responses and early morphological alteration signaling. BioRxiv Prepr Serv Biol. 2025;2025.01.29.635571. doi: 10.1101/2025.01.29.635571.

35. Kim DH, Hong YJ, Lee HJ, Choi BY, Kim CH, Park JO, Kang JH, Choi BJ, Kim JH, Ahn YM, et al. Immunogenicity and protective effectiveness of Japanese encephalitis vaccine: a prospective multicenter cohort study. Korean J Pediatr Infect Dis. 2013;20(3):131–138. doi: 10.14776/kjpid.2013.20.3.131.

36. Wang M, Hu L, Xu C. Recent advances in the design of polymeric microneedles for transdermal drug delivery and biosensing. Lab Chip. 2017;17(8):1373–1387. doi: 10.1039/C7LC00016B.

37. Sartawi Z, Blackshields C, Faisal W. Dissolving microneedles: applications and growing therapeutic potential. J Control Release Off J Control Release Soc. 2022;348:186–205. doi: 10.1016/j.jconrel.2022.05.045.

38. Moore LE, Vucen S, Moore AC. Trends in drug- and vaccine-based dissolvable microneedle materials and methods of fabrication. Eur J Pharm Biopharm Off J Arbeitsgemeinschaft Pharm Verfahrenstech EV. 2022;173:54–72. doi: 10.1016/j.ejpb.2022.02.013.

39. Chen Y, Alba M, Tieu T, Tong Z, Minhas RS, Rudd D, Voelcker NH, Cifuentes-Rius A, Elnathan R. Engineering micro–nanomaterials for biomedical translation. Adv NanoBiomed Res. 2021;1(9):2100002. doi: 10.1002/anbr.202100002.

40. Park J-H, Allen MG, Prausnitz MR. Biodegradable polymer microneedles: fabrication, mechanics and transdermal drug delivery. J Control Release Off J Control Release Soc. 2005;104(1):51–66. doi: 10.1016/j.jconrel.2005.02.002.

41. Sachdeva KS, Chadha VK. TB-Vaccines: current status & challenges. Indian J Med Res. 2024;160(3–4):338–345. doi: 10.25259/IJMR_1478_2024.

42. Lawrence A. Bacillus Calmette-Guérin (BCG) revaccination and protection against tuberculosis: a systematic review. Cureus. 16(3):e56643. doi: 10.7759/cureus.56643.

43. Lai R, Ogunsola AF, Rakib T, Behar SM. Key advances in vaccine development for tuberculosis—success and challenges. NPJ Vaccines. 2023;8(1):158. doi: 10.1038/s41541-023-00750-7.

44. Lang R. Recognition of the mycobacterial cord factor by Mincle: relevance for granuloma formation and resistance to tuberculosis. Front Immunol. 2013;4:5. doi: 10.3389/fimmu.2013.00005.

45. Imai T, Matsumura T, Mayer-Lambertz S, Wells CA, Ishikawa E, Butcher SK, Barnett TC, Walker MJ, Imamura A, Ishida H, et al. Lipoteichoic acid anchor triggers mincle to drive protective immunity against invasive group a streptococcus infection. Proc Natl Acad Sci USA. 2018;115(45):E10662–E10671. doi: 10.1073/pnas.1809100115.

46. Gutiérrez-Martínez E, Planès R, Anselmi G, Reynolds M, Menezes S, Adiko AC, Saveanu L, Guermonprez P. Cross-presentation of cell-associated antigens by MHC class I in dendritic cell subsets. Front Immunol. 2015;6:363. doi: 10.3389/fimmu.2015.00363.

47. Wozniak TM, Saunders BM, Ryan AA, Britton WJ. Mycobacterium bovis BCG-Specific Th17 cells confer partial protection against mycobacterium tuberculosis infection in the absence of gamma interferon. Infect Immun. 2010;78(10):4187–4194. doi: 10.1128/IAI.01392-09.

48. Shen H, Chen ZW. The crucial roles of Th17-related cytokines/signal pathways in M. Tuberculosis infection. Cell Mol Immunol. 2018;15(3):216–225. doi: 10.1038/cmi.2017.128.

49. Garcia-Pelayo MC, Bachy VS, Kaveh DA, Hogarth PJ. BALB/c mice display more enhanced BCG vaccine induced Th1 and Th17 response than C57BL/6 mice but have equivalent protection. Tuberc (Edinb). 2015;95(1):48–53. doi: 10.1016/j.tube.2014.10.012.

50. Rungelrath V, Ahmed M, Hicks L, Miller SM, Ryter KT, Montgomery K, Ettenger G, Riffey A, Abdelwahab WM, Khader SA, et al. Vaccination with mincle agonist UM-1098 and mycobacterial antigens induces protective Th1 and Th17 responses. NPJ Vaccines. 2024;9(1):1–15. doi: 10.1038/s41541-024-00897-x.

51. Nemes E, Khader SA, Swanson RV, Hanekom WA. Targeting unconventional host components for vaccination-induced protection against TB. Front Immunol. 2020;11:1452. doi: 10.3389/fimmu.2020.01452.

52. Imai N, Tawara I, Yamane M, Muraoka D, Shiku H, Ikeda H. CD4 + T cells support polyfunctionality of cytotoxic CD8+ T cells with memory potential in immunological control of tumor. Cancer Sci. 2020;111(6):1958–1968. doi: 10.1111/cas.14420.

53. Chesson CB, Huante M, Nusbaum RJ, Walker AG, Clover TM, Chinnaswamy J, Endsley JJ, Rudra JS. Nanoscale peptide self-assemblies boost BCG-Primed cellular immunity against mycobacterium tuberculosis. Sci Rep. 2018;8(1):12519. doi: 10.1038/s41598-018-31089-y.

54. Benedictus L, Steinbach S, Holder T, Bakker D, Vrettou C, Morrison WI, Vordermeier M, Connelley T. Hydrophobic mycobacterial antigens elicit polyfunctional T cells in mycobacterium bovis immunized cattle: association with protection against challenge? Front Immunol. 2020;11:588180. doi: 10.3389/fimmu.2020.588180.

55. Kwon KW, Lee A, Larsen SE, Baldwin SL, Coler RN, Reed SG, Cho S-N, Ha S-J, Shin SJ. Long-term protective efficacy with a BCG-Prime ID93/GLA-SE boost regimen against the hyper-virulent mycobacterium tuberculosis strain K in a mouse model. Sci Rep. 2019;9(1):15560. doi: 10.1038/s41598-019-52146-0.